Molecular Crystals and Liquid Crystals

Publication details, including instructions for authors and subscription information:
http://www.tandfonline.com/loi/gmcl20

Phase Transitions and Characterization in a Chiral Smectic-$A_{deVries}$ Liquid Crystal by Low-Frequency Dielectric Spectroscopy

D. M. Potukuchi [a] & A. K. George [b]

[a] Department of Physics, Jawaharlal Nehru Technological University, College of Engineering, Kakinada, India

[b] Department of Physics, College of Sciences, Sultan Qaboos University, Muscat, Oman

Version of record first published: 31 Aug 2012.

To cite this article: D. M. Potukuchi & A. K. George (2008): Phase Transitions and Characterization in a Chiral Smectic-$A_{deVries}$ Liquid Crystal by Low-Frequency Dielectric Spectroscopy, Molecular Crystals and Liquid Crystals, 487:1, 92-109

To link to this article: http://dx.doi.org/10.1080/15421400802221847

Mol. Cryst. Liq. Cryst., Vol. 487, pp. 92–109, 2008

ISSN: 1542-1406 print/1563-5287 online
DOI: 10.1080/15421400802221847

Taylor & Francis
Taylor & Francis Group

Phase Transitions and Characterization in a Chiral Smectic-$A_{deVries}$ Liquid Crystal by Low-Frequency Dielectric Spectroscopy

D. M. Potukuchi[1] and A. K. George[2]
[1]Department of Physics, Jawaharlal Nehru Technological University, College of Engineering, Kakinada, India
[2]Department of Physics, College of Sciences, Sultan Qaboos University, Muscat, Oman

Low-frequency (10 Hz–6.5 MHz) dielectric investigations are carried out in Smectic-A_{deVr} phase exhibited by a chiral Liquid Crystal molecule viz., TSiKN65F. Phase transition temperature determined by dielectric method agrees with TM and DSC. LF dielectric study revealed two relaxations in SmA^{*}_{deVr} phase, i.e., a Low-frequency sluggish LF-mode and a High-frequency fast HF-mode of dipole reorientation. Dynamics estimated through slope of $f_R(T)$ infers faster HF-mode by three orders. The Arrhenius shift of HF-mode f_R infers an activation energy of 0.72 eV. Influence of field on LF mode is studied. Off-centered dielectric dispersion is analyzed through Cole–Davidson equation. Trends of static permittivity (ε_o), high-frequency permittivity (ε_∞), dielectric increment $\Delta\varepsilon$, and α-parameter studied from Cole–Cole plots are explained.

Keywords: activation energy, chiral, de Vries Phase, relaxation, transition temperature

INTRODUCTION

Liquid Crystal (LC) materials possess lucrative electro-optic properties and have gained importance [1–3] among display materials. The critical phenomena associated with the growth of order parameter and fluctuations in the vicinity of the phase transitions are interesting in the area of statistical thermodynamics of these low-dimensional LC systems. Nevertheless, the discoveries of incommensurate (where smectic layer spacing is equal to integeral multiples of length of

Address correspondence to D. M. Potukuchi, Department of Physics, Jawaharlal Nehru Technological University, College of Engineering, Kakinada 533003, India. E-mail: potukuchidm@yahoo.com

molecule) and frustrated smectic phases (explained on the base of soliton propagation) along with the randomly (i.e., localized to the layer) ordered (tilt) deVries phases (explained by Diffuse Cone model viz., DC model) renewed [4] the fundamental aspect of interest in LCs. The important structural aspect of the deVries phase is that it is accompanied with no-layer shrinkage phenomena, in spite of the finite tilt (in their smectic version). As such, the corresponding study of critical dynamics, growth of order parameter and fluctuations at the phase transitions in DeVries Liquid Crystals (DLCs) remained intriguing. The relevance of DC-model and its implications are analyzed through the rigorous [5,6] experimental investigations subsequently. However, the advent of ferroelectricity [7] in tilted smectic phase (i.e., SmC^*) exhibited by chiral LC molecules and their fast (nanosecond) Electro-Clinic [8] response (EC-effect in SmC^* and SmA^* phases) accelerated the design and high-resolution investigations [9,24] in the chiral deVries phases as to optimize their utility. The electroclinic effect in these chiral deVries phases is reported to be larger [11,12,14,17] than that found in their achiral analogs. It is also noticed that the deVries behavior is reported [10] even in the antiferroelectric (AF) phase exhibited by chiral LC molecules. The occurrence of:

a) No-layer shrinkage in $SmC^*_{deVries}$ phase (possessing long range random tilt); and
b) Orthogonal SmA^*_{deVr} phase with random tilt within the smectic layer

in chiral LC molecules is addressed (in chiral deVries LCs, i.e., in CDLCs) through [12] the Asymmetric Diffuse Cone (ADC) model. As the X-ray reflections relevant to the cone (reflecting overall tilt direction over the layers in book-shelf geometry) are diffuse, it's severe vulnerability to the external field is anticipated. A large EC-effect can be expected. This large induced tilt (by the applied field) results for a higher contrast ratio and wider viewing angle. With a strong interest to realize the large EC-effect at ambient temperatures, LC researchers shifted [23,24] their interests for the design of DLC materials (involving heavy fluorination and by proper configuring of the siloxane moiety at the ends of the molecule or as back-bone onto the molecular frame). A large number of experimental investigations reported [9,24] in these chiral DLCs discussed the applicability of DC and ADC models.

An overview of experiments reported in deVries phases uniquely speak out of the fast switching and large EC-effect as an interesting aspect of these materials. Since the DLCs are also reported

[12,13,15–17,20,22] to exhibit equivalently strong EC-response in their SmA version (i.e., in SmA^*_{deVr} phase also), the details of their dielectric response (especially in LF region) is expected [25,26] to provide invaluable information regarding the underlying microscopic interactions as to optimize their utility in electro-optic (EO) displays.

The SmC^* phase is known [27] to exhibit $C_{2\otimes}$ symmetry. A tilde is used denote random tilt. As far as phase symmetry is concerned, SmC^*_{deVr} is distinguished from SmA^*_{deVr} phase through the $C_{\tilde{2}\otimes}$ symmetry being overall in the former case, while it reduces to local symmetry (within the layer) in the latter case.

Low-frequency (LF) dielectric (5 Hz–10 MHz) investigations in the thermotropic LCs are long known [26,28–31] to detect the phase transitions and to understand the response of dipole moment (to the field) which is inherently anisotropic in LCs. However, this interaction of electric field and dipole is manifested through their (individual [28,31] or collective [32,36]) dipolar response. As such, the dielectric results are useful to optimize the LCs in EO devices. It is also noticed that LF dielectric investigations are rather scantily reported [23,24] in SmA or SmC phases exhibited by chiral DLCs. Usually, the off-centered LF dielectric dispersion in LCs is analyzed through the Cole-Davidson [37] relation.

In this article, we present the experimental results of LF (5 Hz–13 MHz) dielectric investigations in a chiral deVries LC, viz., TSiKN65F. This DLC compound is reported [16] to exhibit isotropic to SmA^*_{deVr} phase transition along with a large EC-effect.

EXPERIMENTAL

The DLC viz., TSiKN65F is synthesized following the earlier reported [16] procedure. The molecular formula and the configuration of longitudinal (μ_l) and transverse (μ_t) dipole moment are illustrated in Template-1. The Device Tech made 10 μm spaced cells (made up of transparent glass plates which are buffed with a polymer over the conductive coating to ensure alignment of sample between the plates) were used for LF dielectric studies. An HP LF 4192A Impedance Analyzer was used in conjunction with an HP 16047 C test-fixture kit during the LF dielectric experiments. The leads of the cell are connected to LF Impedance Analyzer which is operated with $1V_{p\text{-}p}$ oscillating signal. The capacitance C and dielectric loss factor TanΔ were recorded from panel-I and panel-II of the instrument, respectively. The LC cell was kept in a PC monitored Instec temperature controller. The accuracy of temperature measurement was ± 0.01 K. An AR grade Benzene (from Fischer) was used for the calibration of the dielectric cell to determine the lead capacitance.

RESULTS AND DISCUSSION

The capacitance of empty cell at RT (room temperature) is found to be small ($\sim$140 pF) in comparison with the value of capacitance exhibited by the cell ($\sim$350 pF) filled with TSiKN65F. Further, capacitance of the empty cell is found to be almost invariant ($<1\%$ variation) with temperature (in the range of 25–100°C) and frequency (in the range of 20 Hz–7.5 MHz with a value of 2.42 pF). The lead capacitance is also found to be constant with temperature and frequency (in the temperature and frequency ranges of interest). The empty cell is filled with LC in its high temperature isotropic state (at 80°C) by capillary action. LF Impedance Analyzer and is excited with $1V_{p\text{-}p}$ oscillating signal at 100 KHz frequency. The temperature of the LC cell is decreased and the corresponding observations of capacitance and loss factor TanΔ of the empty and cell filled with LC are recorded. The dielectric constant (or relative permittivity ε_r) exhibited by LC material at any temperature is estimated from the following formula

$$\varepsilon_r = [C_{DLC} - C_{leads}]/[C_{empty} - C_{leads}] \quad (1)$$

where C_{leads} and C_{empty} are the values of capacitance observed during the calibration (using the AR grade Benzene) process.

I-SmA$^*_{deVr}$ Phase Transition Temperature

It is observed that the dielectric constant ε_r(T) exhibited by TSiKN65F (DLC material) is found (Fig. 1) to increase as SmA$^*_{deVr}$ grows by decreasing temperature. Increase in ε_r reflects the increasing structural correlation of the dipole moment as the SmA$^*_{deVr}$ phase grows in isotropic liquid. The increasing trend of ε_r is found to accompany with a peak value at 67.98°C. The temperature at which ε_r exhibits a peak is identified as the $T_{IS0\text{-}A^*deVr}$ transition temperature for TsiKN65F. However, the phase transition temperature is more clearly identified by plotting the derivative of dielectric constant, i.e., $d\varepsilon_r/dT$ is plotted (Fig. 1) with temperature. $d\varepsilon_r/dT$ is also found to exhibit a peak at a specified temperature. The temperatures at which $d\varepsilon_r/dT$ exhibits a peak is considered as isotropic to SmA$^*_{deVr}$ phase transition temperature. The Isotropic-SmA$^*_{deVr}$ phase transition temperature determined by dielectric method is found to agree with the reports [16] by TM and DSC methods.

Dielectric Dispersion

The capacitance C(ω) and loss factor TanΔ(ω) exhibited by LC in its SmA$^*_{deVr}$ phase are studied (as a function of frequency) at different

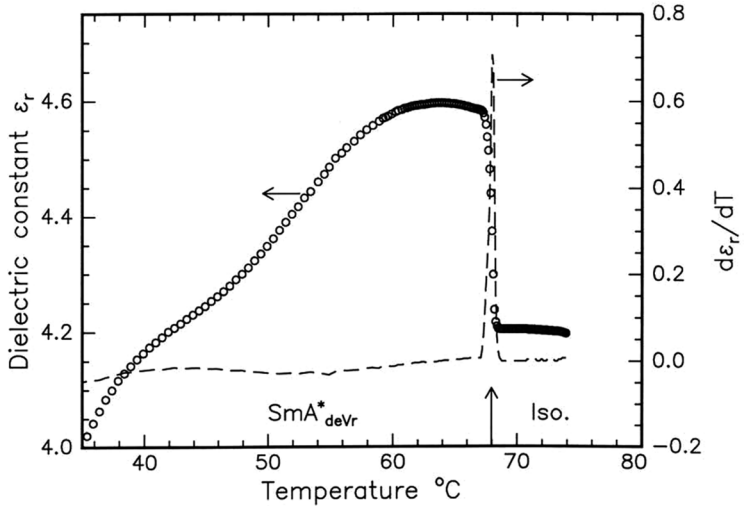

FIGURE 1 Temperature variation of Relative permittivity ε_r(T) and its derivative $d\varepsilon_r/dT$ exhibited by TSiKN65F.

temperatures. The dielectric constant (or relative permittivity) $\varepsilon_r(\omega)$ is estimated from the data of C(ω) with the help of Eq. (1). It is found that ε_r exhibits a monotonical decrease with frequency. The dielectric loss factor Tan$\Delta(\omega)$ studied (at a specified temperature is presented as a representative in Fig. 2) in SmA^*_{deVr} phase is found to exhibit two (clearly appear as additional peaks when superposed over the Tan$\Delta(\omega)$ exhibited by empty cell as presented in Fig. 2) peaks. A large peak in TanΔ is noticed at a frequency of $\sim$100 Hz. A small peak is also noticed at a frequency of $\sim$4 MHz. Although the HF-peak is observed to be small (and broad), this peak becomes strikingly distinguishable, when viewed (Fig. 2) against the back ground of the TanΔ exhibited by empty cell. It is also noticed that TanΔ exhibited by LC in SmA^*_{deVr} phase increases towards the HF end (i.e., for frequency $\geq$6 MHz) and/or towards the lower (for frequency $\leq$50 Hz) end. Similar increasing trend of TanΔ is found to be exhibited by empty cell (dotted line in Fig. 2) also. This increase of TanΔ (by both the LC filled cell and empty cell at the $<$40 Hz and $>$6 MHz) is interpreted [32] as due to the contribution of conductive coating and trace level ionic impurities in the cell.

The complex dielectric constant of a material under the influence of ac fields is given by

$$\varepsilon^*(\omega) = \varepsilon'(\omega) - j\varepsilon''(\omega),$$

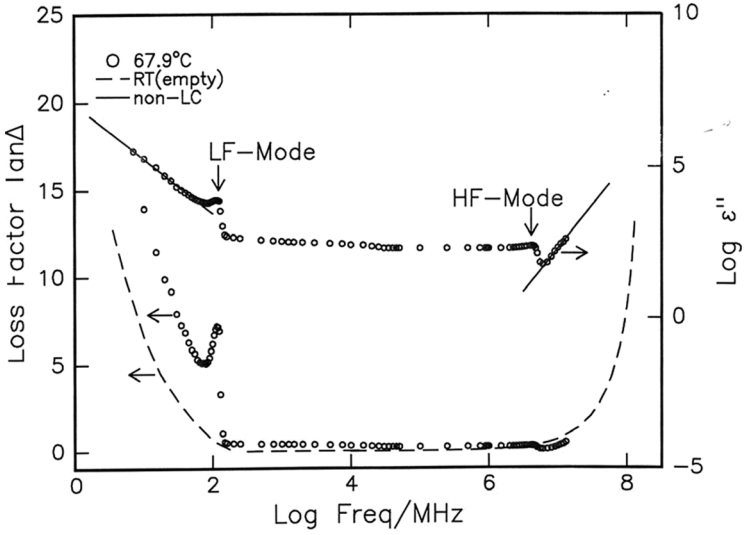

FIGURE 2 Frequency (in MHz) variation of loss factor TanΔ and loss ε'' exhibited by TSiKN65F cell and empty cell at RT($\sim$25°C) in SmA^*_{deVr} phase.

where the real part of the dielectric constant ε' is frequently identified as experimentally measurable relative permittivity ε_r.

The dielectric loss $\varepsilon''(\omega)$ is estimated from the data of $\text{Tan}\Delta(\omega)$ (corresponding to an applied $1\,V_{p\text{-}p}$ sine wave) using the equation given by

$$\varepsilon''(\omega) = \varepsilon_r(\omega) * \text{Tan}\Delta(\omega), \tag{2}$$

where $\varepsilon_r(\omega)$ value is estimated from the observed Capacitance and TanΔ values using Eq. (1).

In order to resolve the relaxation processes exhibited by LC with that of the contributions from the conductive coating (or trace level ionic impurities), a standard procedure is applied [32] by fitting the dielectric data to a relation given by

$$\varepsilon'' \propto f^d.$$

A Log-Log plot (as a representative plot) is drawn for observed ε'' versus frequency (Fig. 2 for right side y-axis) distribution exhibited by the DLC in its SmA^*_{deVr} phase. The slopes (i.e., shown by the inset solid lines superposed over the observed data) of the plot are found to be -1.015 and 0.95 for the regions viz., $<50\,Hz$ and $>5\,MHz$, respectively. The values of slope is found to agree with the reported [32] values. Therefore, the increase of TanΔ for $<50\,Hz$ and

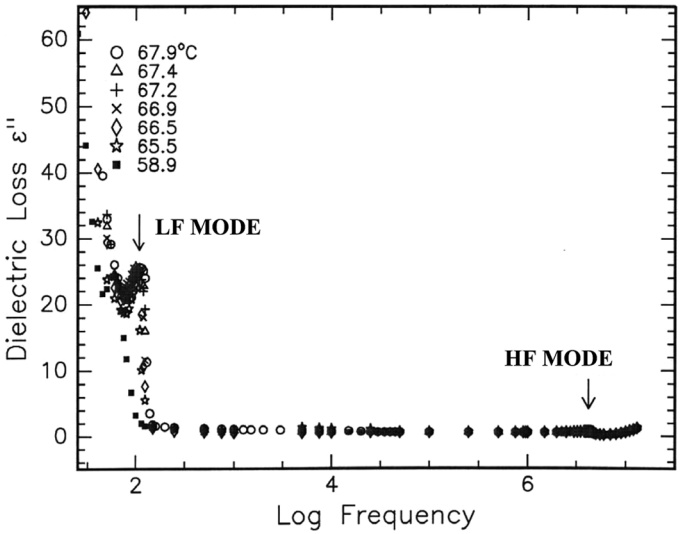

FIGURE 3 Frequency (in MHz) variation of dielectric loss $\varepsilon''(\omega)$ exhibited by DLC in SmA^*_{deVr} phase at different temperatures.

>5 MHz is confirmed as due to trace level ionic impurities and ITO conductive coating on the plates, respectively. In the wake of these slope values (of these log-log plots) and the observed TanΔ (exhibited by the LC) superposed over that of empty cell in Fig. 2, it is confirmed that the two peaks in loss are due to two relaxations viz., LF-mode at $\sim$100 Hz and HF-mode $\sim$4 MHz exclusively contributed by the LC material as a response to the field.

The dielectric loss observed at different temperatures in the SmA^*_{deVr} is presented in Fig. 3. As per the Debye's theory [25,26] each peak in loss spectra i.e., $\varepsilon''(\omega)$ refers to a relaxation process. Usually, a relaxation process involves the reorientation of dipole moment to the field. As LC molecule possesses anisotropic dipole moment, the reorientation and relaxation time scale differs as per the nature and configuration of the component that responds to field. However, the frequency at which ε'' attains peak value (in the observed the loss spectrum ε'') is considered as the relaxation frequency f_R. The time scale of relaxation process, i.e., $1/f_R$ differs for different components of μ. A meticulous observation of Fig. 3 reveals the shift of f_R with temperature in both the cases of LF and HF relaxations observed in SmA^*_{deVr} phase. For clarity, the shift of f_R with temperature is redrawn as Figs. 4 and 5 (by confining the variation of ε'' around it's peak) for LF and HF-modes, respectively. The results of $Tan\Delta_{max}$,

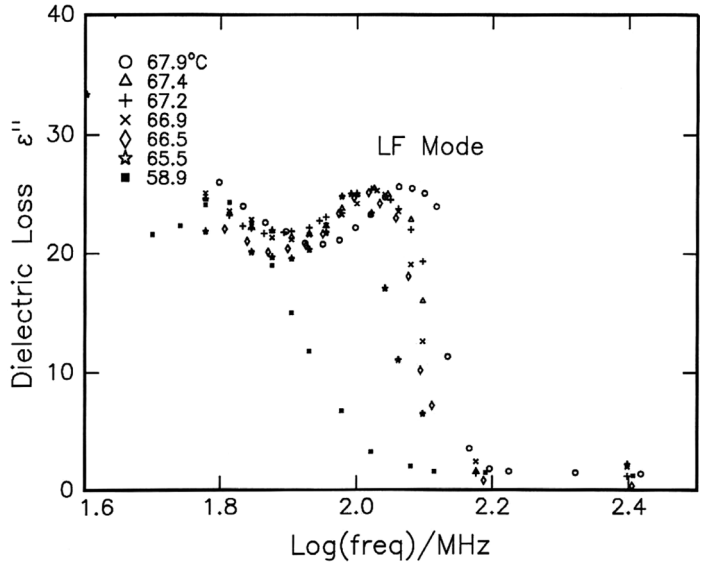

FIGURE 4 Frequency (MHz) variation of dielectric loss $\varepsilon''(\omega)$ to study the temperature shift of relaxation frequency f_R regarding LF LF mode.

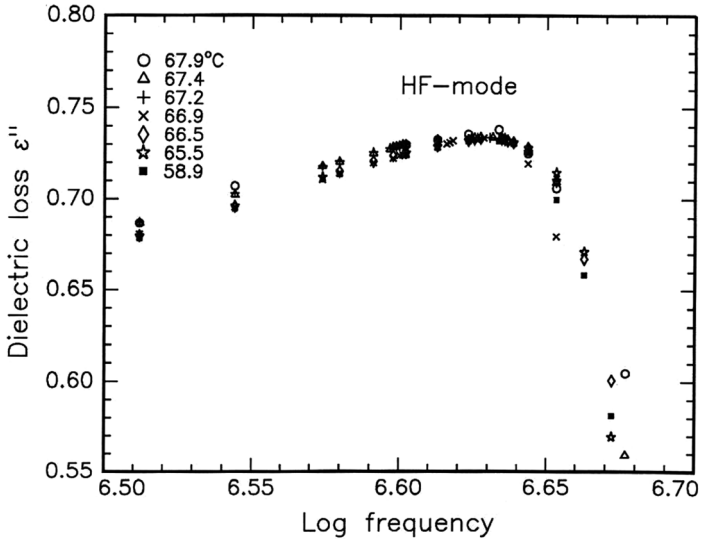

FIGURE 5 Frequency (in MHz) variation of dielectric loss $\varepsilon''(\omega)$ projected to study temperature shift of relaxation frequency f_R regarding HF-mode.

TABLE 1 Data of Relaxation frequency (f_R), Relaxation Time τ_R, Maxima of Loss Factor $Tan\Delta_{max}$, Maxima of Dilectric Loss ε''_{max} Relevant to LF and HF Relaxations in $SmA^*_{deVries}$ LC Phase

	LF- mode				HF-Relaxation			
Temp. in °C	Relaxation frequency f_R in Hz	τ in ms.	$Tan\Delta_{Max}$	ε''_{max}	Relaxation frequency f_R in MHz	τ in ms.	$Tan\Delta_{Max}$	ε''_{max}
67.9	115	8.69	7.212	25.650	4.30	0.232	0.29390	0.7343
67.4	111	9.0	6.954	25.410	4.28	0.233	0.29220	0.7341
67.2	110	9.01	6.818	25.406	4.27	0.234	0.29215	0.73398
66.9	107	9.3	6.661	25.320	4.25	0.235	0.29210	0.73398
66.5	104	9.6	6.498	25.152	4.24	0.235	0.29200	0.7337
65.5	98	1.0	6.139	25.050	4.23	0.236	0.29180	0.7332
58.9	65	1.5	4.496	24.307	4.30	0.238	0.29140	0.73219

ε''_{max} and f_R observed for the LF and HF relaxations are presented in Table 1. Although, f_R for LF mode is relatively lower, it's range in SmA^*_{deVr} phase falls in the same order of f_R ($\sim$100 Hz) reported [32–35] for the Goldstone mode (viz., GM) in FE SmC^* phase. However, the present LF mode f_R falls on the lower side of the reported values for GM in FLCs. Further, the ε''_{max} observed for LF mode in SmA^*_{deVr} phase attains a very large (as large as $Tan\Delta_{max} \sim 7.25$ and $\varepsilon''_{max} \sim 25$) value in comparison with the values reported [32,35] for the GM in SmC^*. It is also noticed that the large loss (and lower f_R) observed in the TSiKN65F are found comparable to the reported [23,24] loss values in the SmA^*_{deVr} phase regarding its Phason mode. As, the present DLC (viz., TSiKN65F) possesses (in Template 1) a chiral centre, presently observed LF mode is considered as collective response (of transverse dipole moment). The orthogonally structured SmA phase assumes with a finite (and nonzero) but, random tilt (within the layer) in the present SmA^*_{deVr} phase. Local tilt within SmA^* layers is a characteristic feature of deVries phase. Hence, the mechanism behind the present LF mode is argued as the excitation of the coupled transverse dipole moment μ_t (situated in the vicinity of the chiral centre). The tilt in SmA^*_{deVr} phase is local (while it is long range in SmC^* phase). As such, the situation leads to a weaker (than in SmC^*) coupling of μ_t in SmA_{deVr} phase. The weak (or partial) coupling in turn also manifests in the form of weak polarization helix. Hence, the present case of LF relaxation in SmA^*_{deVr} phase needs further analysis. Since LF relaxation is considered as due to the collective

response, the temperature variation of f_R is not considered as Arrhenius shift for the calculation of activation energy.

The mechanism behind the high HF-relaxation ($f_R \sim 4$ MHz) is interpreted as due to a process involving the reorientation of dipole (i.e., longitudinal dipole-moment μ_1 situated along aromatic rigid core region of molecule (as pictured in Template-1) to the field. It is also noticed that similar Multiple relaxation phenomena is explained [28,29] through a resolved dipole model in the case of achiral smectic LCs. The higher f_R corresponding to the present HF (MHz) relaxation is explained as due to the fast reorientation longitudinal dipole moment (i.e., fast response of dipole situated at rigid core part of molecule) to the field. Since the μ_1 is situated in the aromatic rigid core part of the molecule, the viscous drag it experiences in the dielectric medium is less. Therefore, it can readily follow the field (i.e., at higher frequencies). Hence, the reorientation process results as faster. The observed shift of f_R with temperature (for HF relaxation) is viewed as Arrhenius shift, since it is a case of response of individual dipole moment to the filed. The activation energy reflects upon the potential barrier experienced by the dipole during its reorientation to the field. The activation energy estimated (Fig. 6) through reduced temperature plot (from the observed data of f_R *versus* T) in the case of HF relaxation yielded 0.72 eV. The estimated activation energy falls rather on the

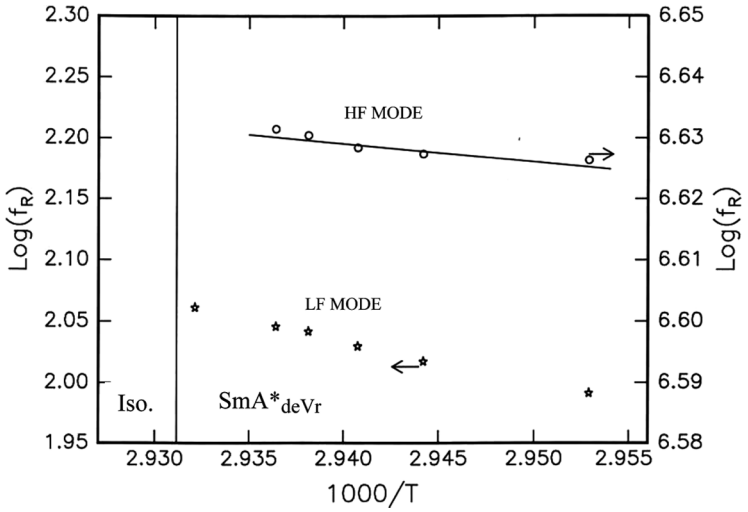

FIGURE 6 Temperature (kK^{-1}) dependence of f_R (in MHz) for LF and HF relaxations exhibited by TSiKN65F in SmA^*_{deVr} phase for activation energy.

higher side of the reported [31,38] values in the LCs (in their smectic or nematic phases). The higher value of activation energy in the present deVries LC is argued as due to the presence of siloxane spacer and chiral center (as μ_1 on the molecular frame with additional constraints) during its reorientation to the field.

Dynamics

The growth and time evolution of SmA^*_{deVr} phase as manifested through the resolved dipole moment (HF and LF-collective dipole response) is studied in the following way.

A comparison is drawn between the collective (LF) mode and individual (HF) mode dynamics (exhibited by the DLC in its SmA^*_{deVr} phase in the thermal range of 3°C below the isotropic to SmA^*_{deVr} phase transition) by estimating the slope of $f_R(T)$ in Table 1. The estimated df_R/dT (in a thermal span of 2.4°C) regarding LF mode is found to be $7.083\,Hz{\cdot}K^{-1}$, while that for HF is found to be $2.92 \times 10^4\,Hz{\cdot}K^{-1}$. The large value of slope of $f_R(T)$ is attributed to the fast dynamics involved with the individual dipole response.

Relative dipole dynamics is further analyzed through study of temperature variation of relaxation time (Table 1). T_N being the Normalized Temperature is estimated in the range of 2.4°C below the $T_{I\text{-}A^*deVr}$ from the equation given by

$$T_N = [T_{IA^*} - T_1]/[T_{IA^*}].$$

The Normalized Relaxation Time τn is estimated from

$$\tau = 1/f_R \quad \text{and} \quad \tau_N = [\tau_r \text{ at } T_{1-A^*deVr}]/[\tau_i], \quad \text{i.e.,} \, \tau_N = (0.00869)/(\tau_i),$$

where τ_i is the reciprocal of f_R at the temperature of interest. It is noticed that reciprocal of τ_i at $T^*_{I\text{-}smA}$ is equal to 0.00869 s (i.e., the observed values of f_R at 67.98°C is taken as that at T_{IA^*deVr}).

The exponentially decaying distribution of τ_N over $\mathbf{T}_N$ is plotted in Fig. 7. The data is fitted to an exponential relation, as projected by the solid line superposed over the observed data in the thermal range of 2.4°C below the $T_{I\text{-}A^*deVr}$. The yield of exponents β in LF and HF processes are found to be equal to 21.5 ± 0.004 and 5.0 ± 0.0001 for LF mode and HF modes, respectively. The relatively higher value of exponent β (by almost one order) relevant to LF mode reflects upon the sluggish (by one order) collective response than that of HF-relaxation.

A careful observation of ε'' (variation with frequency) exhibited by the deVries LC in SmA^* phase (at different temperatures regarding LF and HF modes presented in the Figs. 4 and 5, respectively) reveals

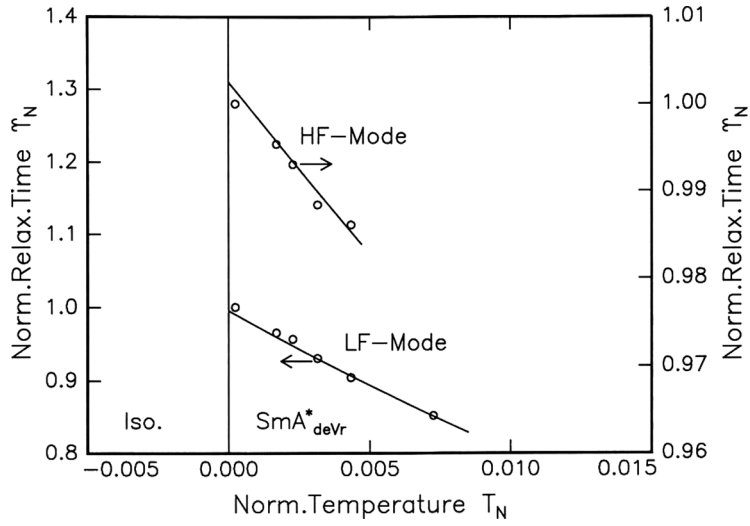

FIGURE 7 Dynamics for LF and HF modes in the vicinity of I-SmA* transition for TSiKN65F.

that the distribution of dielectric loss (about the ε'' peak) is not symmetrical. Hence, the observed dispersion is treated as the case of off-centered. As such, the dispersion is analyzed through Cole-Davidson relation [37] given by

$$\varepsilon^*(\omega) = \varepsilon_\infty(\omega) - [(\Delta\varepsilon)]/[1 + (\mathbf{j}\omega\tau)^{1-\alpha}], \tag{3}$$

where $\omega = 2\pi f$, $\tau = 1/f_R$

$$\Delta\varepsilon = [\varepsilon_o - \varepsilon_\infty]$$

α - Distribution parameter specifying degrees of freedom experience by dipolemoment μ_t during its re-orientation.

ε_∞- is the value of high frequency permittivity end

ε_o - is the value of low frequency permittivity end

estimated from Cole-Cole plots (i.e., ε'' *versus* ε_r drawn corresponding to the observed dispersion at different temperatures).

The Cole-Cole plots corresponding to the LF and HF-modes are presented in Figs. 8 and 9, respectively. The estimated values of static (ε_o) and high frequency (ε_∞) dielectric permittivity, dielectric increment (i.e., $\Delta\varepsilon = \varepsilon_o - \varepsilon_\infty$), and α -parameter are presented in Tables 2 and 3, respectively. It is noticed that the temperature shift of dispersion is effectively tuned through lower frequency (ε_o) side in the case of the LF mode. But, in the case of HF mode, the shift seems to be tuned

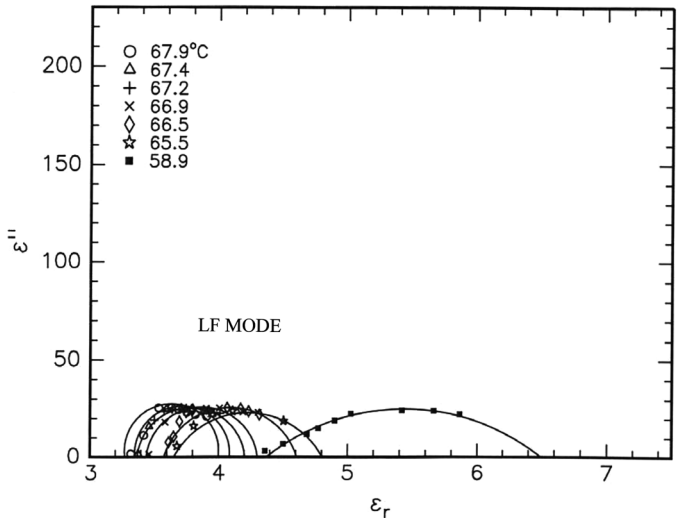

FIGURE 8 Cole-Cole plots for LF mode in the SmA^*_{deVr} phase for TSiKN65F.

through high frequency (i.e., through permittivity ε_∞) side (as observed in Figs. 8 and 9). The predominant static (LF) response regarding the LF mode is attributed to the involvement of collective

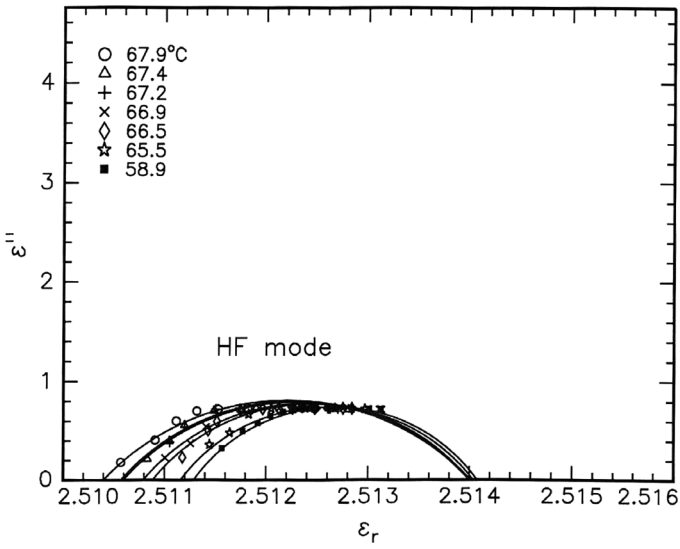

FIGURE 9 Cole-Cole plots HF-mode in the SmA^*_{deVr} phase for TSiKN65F.

TABLE 2 Data of α -Parameter, Static Permittivity ε_o, High-Frequency Permittivity ε_∞, and Dielectric Increment Estimated from Cole-Cole Plots at Different Temperatures for LF-mode in SmA^*_{deVr} LC phase

Temp. in°C	$\alpha \times 10^{-1}$	ε_o	ε_∞	$\Delta\varepsilon$
67.9	0.0001	4.000	3.273	0.727
67.4	0.1047	4.105	3.351	0.754
67.2	0.1396	4.203	3.371	0.832
66.9	0.1745	4.300	3.439	0.861
66.5	0.2094	4.600	3.576	1.024
65.5	0.2268	4.805	3.660	1.145
58.9	0.5059	6.500	4.389	2.111

response. The dielectric increment $\Delta\varepsilon$ is found to increase with decreasing in temperature in the case of LF mode. The LF mode relevant $\Delta\varepsilon$ values are found to bear higher values than those observed with HF mechanism. Collective response corresponding to LF is argued to lead for the observed higher dielectric increment. The distribution parameter (α -values) is found (Tables 2 and 3) to decrease with temperature for both the LF and HF-modes. The decrease in α -parameter with temperature reflects upon the growth of relatively confined dipole (responding either individually or collectively) on the molecular frame.

Influence of External Field on LF Mode

In the wake of the analogy between the the present LF mode (in $SmA^*_{deVries}$ phase) and the GM reported [32,35] in SmC^* phase, it is proposed to study the influence of applied field on the latter case. As

TABLE 3 Data of α -Parameter, Static Permittivity ε_o, High-Frequency Permittivity ε_∞, and Dielectric Increment Estimated From Cole-Cole Plots at Different Temperatures for HF-Mode in $SmA^*_{deVries}$ LC Phase

Temp. in°C	$\alpha \times 10^{-1}$	ε_o	ε_∞	$\Delta\varepsilon$
67.9	0.5401	2.51380	2.51040	3.40×10^{-3}
67.4	0.5234	2.51398	2.51059	3.39×10^{-3}
67.2	0.5059	2.51401	2.51060	3.38×10^{-3}
66.9	0.4710	2.51402	2.51080	3.20×10^{-3}
66.5	0.4536	2.51403	2.51090	3.10×10^{-3}
65.5	0.4362	2.51404	2.5111	3.94×10^{-3}
58.9	0.4187	2.51405	2.51114	3.63×10^{-3}

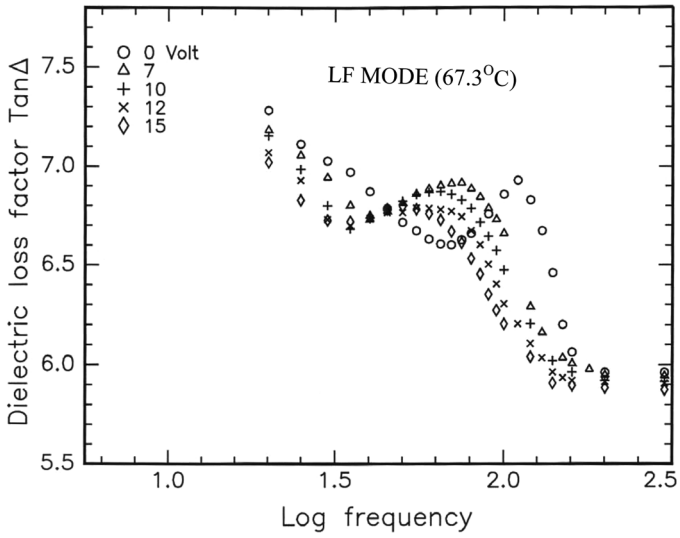

FIGURE 10 Frequency (in MHz) variation of LF-mode TanΔ at different fields observed at 67.3°C.

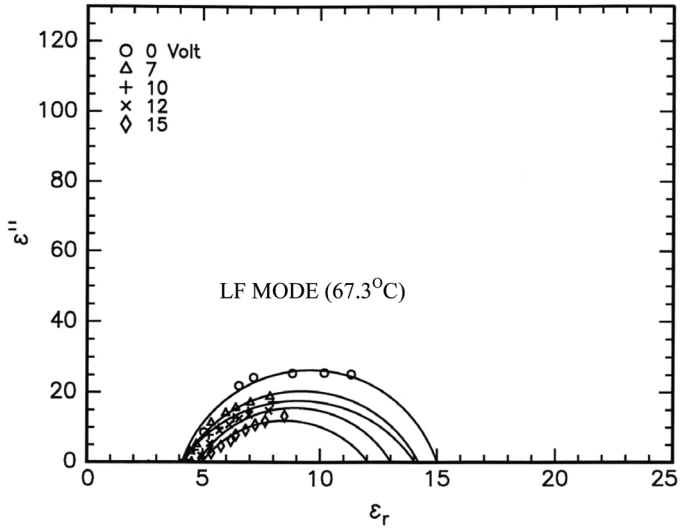

FIGURE 11 Field influence on Cole-Cole plots for the LF mode in SmA_{deVr}^{*} phase for TSiKN65F.

TABLE 4 Data of α -Parameter, Static Permittivity ε_o, High-Frequency Permittivity ε_∞, and Dielectric Increment $\Delta\varepsilon$ Estimated from Cole-Cole Plots of LF-mode Corresponding to Different Field Strengths

Voltage in V	$\alpha \times 10^{-1}$	ε_o	ε_∞	$\Delta\varepsilon$
0	0.20950	15.00	4.25	10.75
7	0.34920	14.25	4.36	09.99
10	0.31428	14.05	4.40	09.65
12	0.38410	13.00	4.60	08.40
15	0.71580	12.00	5.00	07.00

such, the observed LF dielectric dispersion (loss factor TanΔ *versus* frequency) exhibited by the TsiKN65F in SmA^*_{deVr} phase is studied as a function of applied field (i.e., 0 15 V). The results are presented in Fig. 10 (observed at 67.3°C as a representative figure). The corresponding Cole-Cole plots are illustrated in Fig. 11. The estimated values of ε_o, ε_∞, As and the α -parameter are presented in Table 4. It is observed that the dielectric loss factor $Tan\Delta_{max}$ gets reduced (suppressed) with increasing field. This decreasing $Tan\Delta_{max}$ is argued as due to the de-coupling of μ_t over smectic layers. However, the maximum value of loss factor (or peak) is observed to shift to lower frequencies with the increasing field. The shift of $Tan\Delta_{max}$ with bias field is not so appreciable as that observed [32,35] for the GM in SmC^* phase. The observed variation of $Tan\Delta_{max}$ (at different bias corresponding to LF mode relaxation) is presented in Table 5. It is noticed that a threshold field of $\sim$6 v (per 10 μm) is required to start the

TABLE 5 Field Variation of Loss Factor Maxima $Tan\Delta_{max}$ at Different Temperatures for the LF-Mode Relaxation

	Loss factor $Tan\Delta_{max}$				
Field in volts	67.92°C	67.4°C	67.2°C	66.5°C	65.5°C
0	7.215	6.954	6.818	6.498	6.139
2	7.210	6.953	6.810	6.490	6.132
4	7.200	6.952	6.805	6.480	6.128
6	7.180	6.950	6.800	6.475	6.118
8	7.150	6.935	6.775	6.450	6.080
10	7.100	6.925	6.750	6.400	6.030
12	7.000	6.875	6.700	6.350	6.025
14	6.850	6.755	6.000	6.250	6.000
15	6.720	6.700	6.525	6.200	5.980
16	6.600	6.610	6.475	6.150	5.975

de-coupling of the μ_t. It is also interesting to observe that $Tan\Delta_{max}$ retains almost a constant value up to a field of 6v. This behavior is analogous to the observed [24] constant (almost invariant) tilt angle up to an applied field of 30 V during their EC-effect studied in the same compound. It is noticed that the field required to suppress the $Tan\Delta_{max}$ at lower temperature is found to be higher (in magnitude) than that required to suppress it at higher temperature. This infers a relatively strong coupling of μ_t at lower temperatures. The estimated values of ε_o, ε_∞, $\Delta\varepsilon$ and the α -parameter also exhibit a similar trend of variation as observed for the LF and HF-mode relaxations with temperature.

CONCLUSIONS

1. The Phase transition temperature, $T_{I\text{-}A^*deVr}$ determined from LF dielectric studies agree with the TM and DSC values in DLCs.
2. Dielectric dispersion reveals two relaxations in chiral $SmA_{deVries}$ LCs, i.e., an LF mode (viz., a collective response) and a HF-mode (of individual dipole reorientation to the field).
3. Chiral substitution and siloxane spacer on the molecular frame results in the higher activation energy (relevant to HF relaxation).
4. Field variation of dispersion regarding LF mode reveals a subtle and finite threshold field to trigger the switching action in devices made up of chiral deVries LCs.

REFERENCES

[1] Demus, D. (1971). In: *Applications of Liquid Crystals*, Springer Verlag; (1976). *Non-Emissive Electro-Optic Displays*, Knetz, A. R. & Von Willison, F. K. (Eds.), Plenum Press, 94.
[2] Goodby, J. W., Blinc, R., Clark, N. A., Lagerwall, S. T., Osipov, S. A., Pikin, S. A., Sakurai, T., Yushino, Y., & Zeks, B. (1991). In: *Ferroelectric Liquid Crystals, Principles , Properties and Applications*, Gordon & Breach, (Eds.), Philadelphia.
[3] Walba, D. M., Rago, J. A., Clark, N. A., & Shao, R. (1992). In: *Macromolecular Guest-Host Complexes and Optoelectronic Properties and Applications*, Janekhe, A., (Ed.), Pittsburg Material Research Society, *227*, 205.
[4] deVries, A. (1977). In: Abstracts of 5th Intl. Liqd. Cryst. Conference, Stockholm, Brown, G. H. 150 (1974); *ibid. Mol. Cryst. Liq. Cryst. Lettr.*, 42, 27; (1980). *Advances in Liquid Crystal Research and Applications*, Bata, L., (Ed.), Pergamon Press: Oxford, 71.
[5] Diele, S., Brand, R., & Sackmann, H., (1972). *Mol. Cryst. Liq. Cryst.*, 16, 105. deVries, A. (1979). *Mol. Cryst. Liq. Cryst. Lettr.*, *49*, 179; (1979). *J. Chem. Phys*, *71*, 25.
[6] deVries, A., Ekachai, A., & Spielberg, N., (1979). *Mol. Crystl. Liq. Cryst. Lett.*, *49*, 143.
[7] Garoff, S. & Mayer, R. B. (1977). *Phys. Rev. Lett.*, *38*, 848.
[8] Garoff, S. & Mayer, R. B. (1979). *Phy. Rev. A.*, *19*, 338.

[9] Panarin, Y. P., Panar, U., Kalinovskaya, O. E., & Vij, J. K. (1999). *J. Mater. Chem.*, *9*, 2967.
[10] Spector, M. S., Heiney, P. A., Naciri, J., Weslowski, B. T., Holt, D. B., & Shashidhar, R. (2000). *Phy. Rev. E.*, *61*, 1579.
[11] Selinger, J. V., Collings, P. J., & Shashidhar, R. *Phy. Rev. E.*, *64*, 061705.
[12] Mayer, R. B. & Pelkovits, A. (2002). *Phy. Rev. E.*, *65*, 061704.
[13] Clark, N. A., Bellini, T., Shao, R. F., Coleman, D., Bardon, S., Link, D. R., Chen, X. H., Wand, H. D., Walba, D. M., Rudquist, P., & Lagerwall, S. T. (2002). *Appl. Phy. Lett.*, *80*, 4097.
[14] Tang, A., Kanorolov, D., Naciri, J., Ratna, B. R., & Sprunt, S. (2002). *Phy. Rev. E.*, *65*, 010703.
[15] Lagerwall, J. P. F. & Giesselmann, F. (2002). *Phy. Rev. E.*, *66*, 031703.
[16] Naciri, J., Carboni, C., & George, A. K. (2003). *Liq. Cryst.*, *30*, 219.
[17] Kalinovskaya, O. E., Panarin, Y. P., & Vij, J. K. (2001). *Euro. Phys. Lett.*, *57*, 184.
[18] Huang, C. C., Wang, S. T., Han, X. F., Cady, A., Pindak, R., Caliebe, W., Ema, K., Takakoshi, K., & Yao, H. (2004). *Phy. Rev. E.*, *69*, 041762.
[19] Rossle, M., Zentel, R., Lagerwall, J. P. F., & Giesselmann, F. (2004). *Liq. Cryst.*, *31*, 883.
[20] Kruger, M. & Giesselmann, F. (2005). *Phy. Rev. E.*, *71*, 041704.
[21] Hayashi, N., Kato, T., Fukuda, A., Vij, J. K., Panarin, Y. P., Naciri, J., Shashidar, R., Kawada, S., & Kondoh, S. (2005). *Phy. Rev. E.*, *71*, 0414705.
[22] Lagerwall, J. P. F., Coleman, D., Karblova, E., Jones, C., Shao, R., Oton, J., Walba, D. M., Clark, N. A., & Giesselmann, F. (2006). *Liq. Cryst.*, *33*, 17, and the references therein.
[23] Jhakur, A. K., Choudhary, A., Kaur, S., Bawa, S. S., & Biradar, A. M. (2006). *Jr. Appl. Phys.*, *100*, 034104.
[24] Kaeding, A. & Zugenmaier, P. (1998). *Liq. Cryst.*, *25*, 449.
[25] Hill, N. E., Wanghan, W. E., Price, A. H., & Davies, M. (1969). In *Dielectric Properties and Molecular Behaviour*, Von Nostrand: New York, *53*, 554; Jonscher, A. H. (1983). In: "Dielectric Relaxations in Solids", Chelsea Dielectric Press.
[26] Kresse, H. & Miscicki, J. K. (1980). In: *Advances in Liquid Crystal Research and and Applicationss*, Pergamon Oxford press: Pergamon, 287.
[27] Rananavare, S. B., Pisipati, V. G. K. M., & Wong, E. W. (1994). *Phy. Rev. Lett.*, *72*, 3558.
[28] Rani, G. P., Potukuchi, D. M., Rao, N. V. S., & Pisipati, V. G. K. M. (1994). *Solid State Commun.*, *92*, 349; (1996). *Mol. Cryst. Liq. Cryst.*, *289*, 169.
[29] Rani, G. P., Potukuchi, D. M., & Pisipati, V. G. K. M. (1998). *Liq. Cryst.*, *25*, 589.
[30] George, A. K., Al-Hinai, M., Potukuchi, D. M., Al-Harthi, S. H., & Carboni, C. (2003). *Phase Trans.*, *76*, 1035.
[31] George, A. K., Potukuchi, D. M., Al-Harthy, S. H., & Carboni, C. (2004). *Z. Naturforsch.*, *59a*, 659.
[32] Gouda, F., Skarp, K., & Lagerwall, S. T. (1991). *Ferroelectrics*, *113*, 165; Gouda, F., Skarp, K., Lagerwall, S. T., & Kresse, H. (1991). *J. Phys.*, *11*, 167.
[33] Potukuchi, D. M., Goud, B. V. S., & Pisipati, V. G. K. M. (2002). *Ferroelectrics*, *265*, 279; (2003). *Ferroelectrics*, *289*, 77.
[34] Potukuchi, D. M., George, A. K., Carboni, C., Al-Harthy, S., & Naciri, J. (2004). *Ferroelectrics*, *300*, 1.
[35] George, A. K., Al-Hinai, M., Carboni, C., Al-Harthy, S. H., Potukuchi, D. M., & Naciri, J. (2002). *Mol. Cryst. Liq. Cryst.*, *409*, 343.
[36] Chalapathi, P. V., Srinivasulu, M., Goud, B. V. S., Pisipati, V. G. K. M., & Potukuchi, D. M. (2005). *Ferroelectrics*, *325*, 53.
[37] Cole, R. H. & Davidson, D. W. (1952). *J. Chem. Phys.*, *20*, 1389.